Sensitivity Analysis of a 280 – 312 GHz Superheterodyne Terahertz Link Targeting IEEE802.15.3d Applications

Dominik Wrana, Laurenz John, Benjamin Schoch, Sandrine Wagner, and Ingmar Kallfass

***Abstract*—This paper presents the sensitivity analysis of a superheterodyne terahertz link specifically designed for applications using the IEEE802.15.3d standard. With its wide frequency range for LO input signals in conjunction with an IF frequency range spanning over the full E-band, frequency-domain multiplexing of RF channels in the frequency range between 285 and 312 GHz is implemented in line with the frequency standard. In view of determining optimum operating conditions and performance limitations of the MMIC-based THz transmitter and receiver the link is characterized by a back-to-back operation of the transmitter and receiver modules using WR-3.4 waveguide interconnects. Custom E-band frequency extensions provide the intermediate frequency continuous wave or modulated signals with data rates of up to 32 Gbit/s using 32-QAM modulation. The linearity of the presented THz link enables the use of modulation schemes as high as 256-QAM with reduced bandwidths.**

***Index Terms*—wireless communication, THz, transceiver, beyond 5G, IEEE802.15.3d**

I. Introduction

With 5G technologies more and more entering the commercial market, the ever-increasing demand for higher data rates in wireless applications is pushing research activities for future technologies in the context of sixth-generation wireless communication (6G). Possible applications of so-called THz communication systems operating at wireless carrier frequencies around 300 GHz include short-range scenarios like chip-to-chip communication in an industry setting as well as long-range implementations like back- and fronthaul links or fiber extenders as an option for network deployment in remote areas where wired network access is not an option [1]. In all of those scenarios data rates of 100 Gbit/s and beyond are targeted in order to keep up with fiber capabilities. To reach those numbers either higher-order modulation schemes with ultra-high spectral efficiency or lower order modulation schemes in conjunction with large modulation bandwidths are required. The latter are available at frequencies beyond 250 GHz where yet unexploited frequency spectrum is present while simultaneously offering considerably low atmospheric attenuation, which is crucial for long-range transmissions due to the limited power budget of solid-state technologies at such high frequencies. Therefore the WR-3 or H-band, which extends from 220 to 325 GHz, is considered a suitable candidate for future commercialization of high data rate wireless communication. This is reflected in standardization activities of the ITU [2] as well as the IEEE802.15.3d standard [3], with the latter foreseeing either single channels with bandwidths as high as 69.12 GHz or multiple aggregated channels with bandwidths as low as 2.16 GHz in the targeted RF frequency range from 252 to 325 GHz.

Implementation and realization of corresponding wireless communication systems impose stringent requirements on the analog RF frontend components, like e.g. sufficient dynamic range, linearity, spectral purity, and ultra-broadband frequency characteristics. For the implementation of purely electronic frontends compound semiconductor technologies based on InGaAs or InP show advantages with respect to achievable output power, noise performance, and bandwidth but silicon-based technologies like SiGe and CMOS have caught up in terms of achieved data rates [4], [5], [6], [7].

In this work, we focus on integrated superheterodyne transmitter and receiver modules fabricated in a 35 nm InGaAs mHEMT technology with a transit frequency f_t higher than 500 GHz and a maximum frequency of oscillation f_{max} higher than 1 THz [8]. The implemented chipset is specifically designed to comply with the IEEE802.15.3d standard addressing various channels through a large tuning range of the local oscillator (LO) signal as well as a wideband intermediate frequency (IF) interface spanning over the entire E-band. The latter enables real network integration by use of modems intended for fixed-point terrestrial links based on the ITU-R recommendation [9] and ETSI EN 302 217-2 standard [10] which allocate the frequency bands from 71 to 76 GHz as down-link (DL) and 81 to 86 GHz as up-link (UL). With commercially available millimeter-wave modems with integrated E-band RF frontends a data throughput of up to 20 Gbps per modem pair is achieved using channel bandwidths of up to 2 GHz while applying modulation schemes as high as 1024-QAM [11]. By adopting this frequency range as IF input and output to the THz up- and downconverter, we aggregate several of those modem channels for transmission in the 250 - 325 GHz band.

Dominik Wrana, Benjamin Schoch and Ingmar Kallfass are with the Institute of Robust Power Semiconductor Systems, University of Stuttgart, 70569 Stuttgart, Germany (email: dominik.wrana@ilh.uni-stuttgart.de, benjamin.schoch@ilh.uni-stuttgart.de, ingmar.kallfass@ilh.uni-stuttgart.de)

Laurenz John and Sandrine Wagner are with the Fraunhofer IAF, Fraunhofer Institute for Applied Solid State Physics, 79108 Freiburg im Breisgau, Germany (email: laurenz.john@iaf.fraunhofer.de; sandrine.wagner@iaf.fraunhofer.de)

This work has received funding from Horizon 2020, the European Unions's Framework Programme for Research and Investigation, within project ThoR under grant No. 814523 as well as from Deutsche Forschungsgeimnschaft (DFG) within the Research Unit FOR 2863 METERACOM (Metrology for THz Communications) under grant no. 403579441.

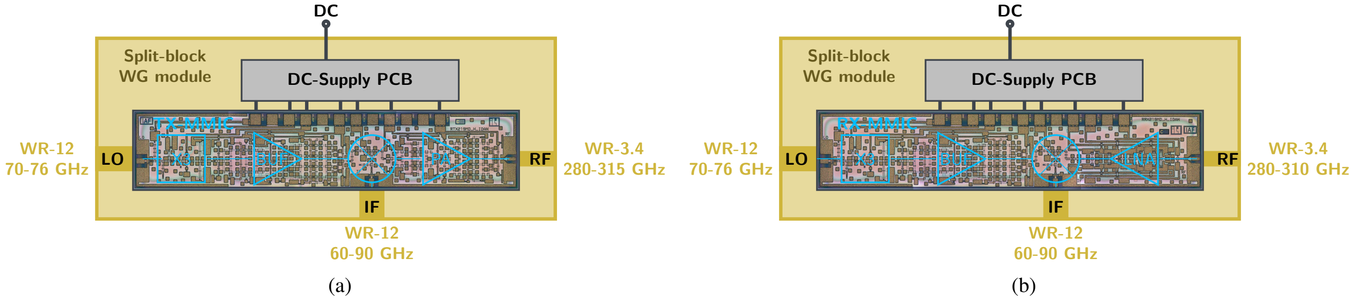

Fig. 1. Block diagrams of the H-band a) transmitter and b) receiver module, each including the MMIC as well as a DC supply PCB which are assembled in a split-block waveguide module.

II. System Architecture

The core hardware components of the superheterodyne link presented in this work are H-band transmitter (Tx) and receiver (Rx) split-block waveguide modules. Targeting applications in compliance with the IEE802.15.3d standard the frontends have been developed with a large IF frequency range expanding over the entire E-band from 60 to 90 GHz, as well as a large LO tuning range in order to address several RF channels. Prior experiments reported in [12] and [13] used other RF hardware to prove the feasibility of the superheterodyne approach at THz frequencies however using considerably low IF frequencies in X-band.

The block diagrams of the split-block waveguide modules containing the frontends implemented in the Tx and Rx MMICs, which use a 35 nm InGaAs m-HEMT technology [8], as well as DC supply circuitry are displayed in Fig. 1 respectively. For both modules, the LO path consists of a times-three frequency multiplier and a buffer amplifier which drives a single-ended resistive fundamental mixer. In case of the Tx the IF signals are directly fed to the upconversion stage which is followed by a five-stage output amplifier in the RF path. A detailed description of the latter one can be found in [14]. On the Rx MMIC, the RF signals are amplified with a three-stage cascode low-noise amplifier (LNA), with measurements of a corresponding breakout circuit showing around 25 dB of small-signal gain, before being down-converted using the identical mixer and LO path present in the Tx circuit. The noise figure of the integrated Rx module could not be measured due to the lack of noise sources, but is expected to lie in the range of 10 dB according to simulation. With the LO as well as the IF frequencies lying in the E-band frequency range, the corresponding module interfaces are realized as WR-12. The RF ports are implemented as WR-3.4 to comply with frequencies in H-band. A description providing more details of the MMIC's building blocks, including on-wafer measurements and a comparison to simulation, is presented in [15].

A. Tx Module

The performance of the Tx versus LO power and frequency is shown in Fig. 2. For all measured LO frequencies saturation of the RF output power P_{RF} is achieved with 3 dBm of LO power. With increasing LO frequency the RF output power

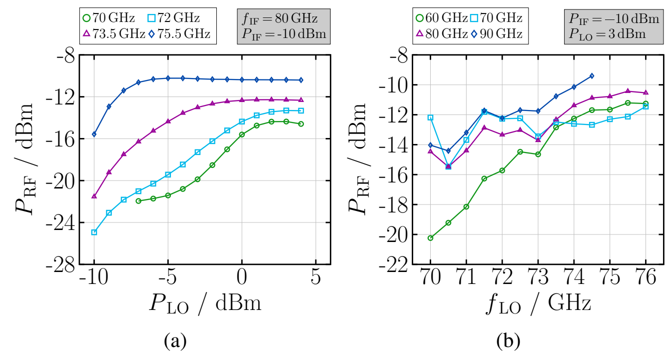

Fig. 2. RF output power of the Tx module versus a) LO input power for different LO frequencies and b) LO frequency for different IF frequencies.

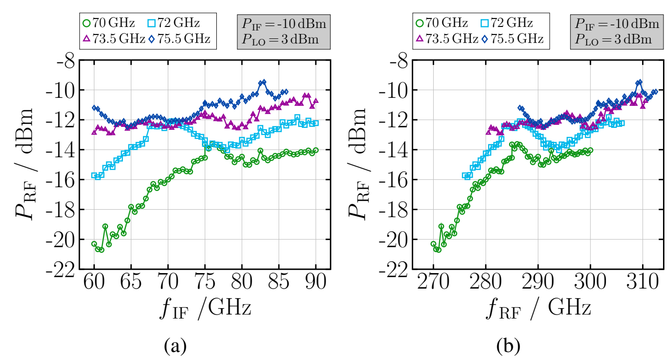

Fig. 3. RF output power of the Tx module versus a) IF input frequency for different LO frequencies and b) RF frequency for different LO frequencies.

P_{RF} increases by approximately 4.5 dB from –14.7 dBm at 72 GHz to –10.2 dBm at 76.5 GHz measured at an IF frequency of 80 GHz and in IF input power of –10 dBm.

As shown in Fig. 3 the Tx achieves an output power P_{out} ranging from –15 to –10 dBm over the IF tuning range from 60 to 90 GHz, measured also at several LO frequencies. Neglecting IF frequencies below 70 GHz in conjunction with LO frequencies below 72 GHz, which lie, as indicated in Fig. 3, at or below the lower passband edge of the RF amplifier, this results in a conversion gain (CG) between –5 and 0 dB considering RF frequencies between 280 and 312 GHz.

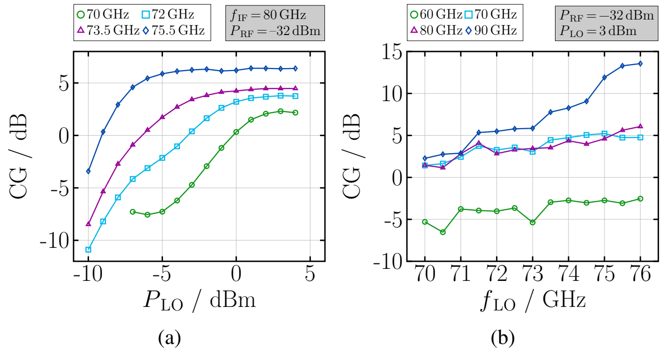

Fig. 4. Conversion gain of the Rx module a) versus LO input power for different frequencies and b) versus LO frequency for different IF frequencies.

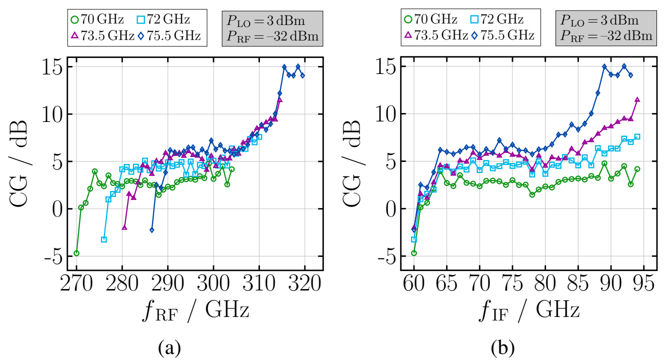

Fig. 5. Conversion gain of the Rx module a) versus RF input frequency for different LO frequencies and b) versus IF output frequency for different LO frequencies.

B. Rx Module

Due to the identical LO path the performance versus LO power for different LO frequencies displayed in Fig. 4 shows comparable behavior to the Tx module with the Rx CG ranging from 2 to 6.5 dB. However, the CG versus LO frequency at a down-converted IF frequency of 60 GHz, which corresponds to RF frequencies in the range between 276 and 289.5 GHz, stays about 6 to 7 dB below the CG for higher IF frequencies.

With respect to the RF bandwidth of the Rx, it is shown in Fig. 5 that a positive conversion gain is achieved from 272 GHz up to 320 GHz. For most of the frequency band, the CG ranges from 5 to 8 dB for LO frequencies of 72 GHz or higher and over the full E-band IF frequency range.

III. Measurement Setup

In the following sections two measurements scenarios for the complete THz link are described which are used to determine on one hand continuous wave (CW) performance metrics like linearity and sensitivity behavior, and on the other hand perform transmission experiments with broadband modulated signals. In both scenarios the H-band transmitter and receiver are operated in a back-to-back configuration as shown in the block diagram in Fig. 6. The RF interface between Tx and Rx is therefore realized by WR-3.4 waveguides in combination with a corresponding tunable attenuator in order to enable an adjustment of the incident RF power for the receiver. The LO signals for the H-band Tx and Rx in the frequency range from 72 to 76.5 GHz are generated using a laboratory-grade electronic frequency synthesizer in conjunction with frequency multiplier modules which implement a multiplication factor of eight. The synthesizer shows a near-carrier phase noise of –110 dBc/Hz at 1 kHz offset frequency and a far-carrier phase noise of –150 dBc/Hz at 100 MHz offset frequency with respect to a output frequency of around 10 GHz. Since both, Tx and Rx modules, require the same LO frequency, the synthesizer output signal is split equally and fed to the respective frequency multipliers via matched cables which results in a coherent LO signal generation. In a real transmission scenario the LO synchronization is performed by modems in the digital domain. Due to the coherent setup the impact of phase noise on signal quality is reduced as the noise for Tx and Rx are identical. The output signals of the multiplier modules are filtered using waveguide bandpass filters with a passband extending over approximately 70 to 76.5 GHz, in order to suppress unwanted harmonics originating from the frequency multipliers. Especially the 7th and 9th harmonics which occur 9 to 9.5625 GHz below and above the wanted 8th harmonic, depending on the desired LO frequency, have to be considered here. In addition, tunable attenuators are used in the LO path to adjust the LO power according to the required power levels for sufficient compression shown in Figs. 2 and 4. In order to comply with all used LO frequencies without having to manually re-adjust the attenuation between measurements the LO power input power is set to 3 dBm for all conducted measurements. To ensure the best possible measurement conditions in all of the used scenarios the arbitrary waveform generator (AWG), frequency synthesizers and the spectrum analyzer or oscilloscope are synchronized via a 10 MHz or 100 MHz reference clock, respectively.

A. CW Setup

In order to extract the CW linearity characteristics of the Tx as well the Rx, a spectrum analyzer in combination with a commercially available E-band frequency extender is used, with the latter one being directly connected to the IF interface of the H-band Rx module. To provide and receive CW as well as modulated signals in E-band to the H-band up-converter, a custom frequency extension is used. Initially designed for up- and down-link applications for future satellite communication [16], the available baseband bandwidth is limited. Targeting applications using the up- and down-link channels of 81 to 86 GHz and 71 to 76 GHz respectively, which have been defined by the ITU [9], the useable 3-dB IF bandwidth extends over approximately 5 GHz resulting in around 10 GHz RF bandwidth. The available linear RF output power of the E-band Tx lies above –5 dBm over the entire available frequency range. To exclude influences of LO leakage and spurious tones, originating from the E-band Tx, which could result in premature transmitter saturation or receiver desensitization, bandpass filters are used to ensure only the wanted test signal being injected to the Tx. A schematic representation of this approach is depicted in Fig. 7 showing the passbands of the two available filters as well as the unwanted LO feedthrough and the upper

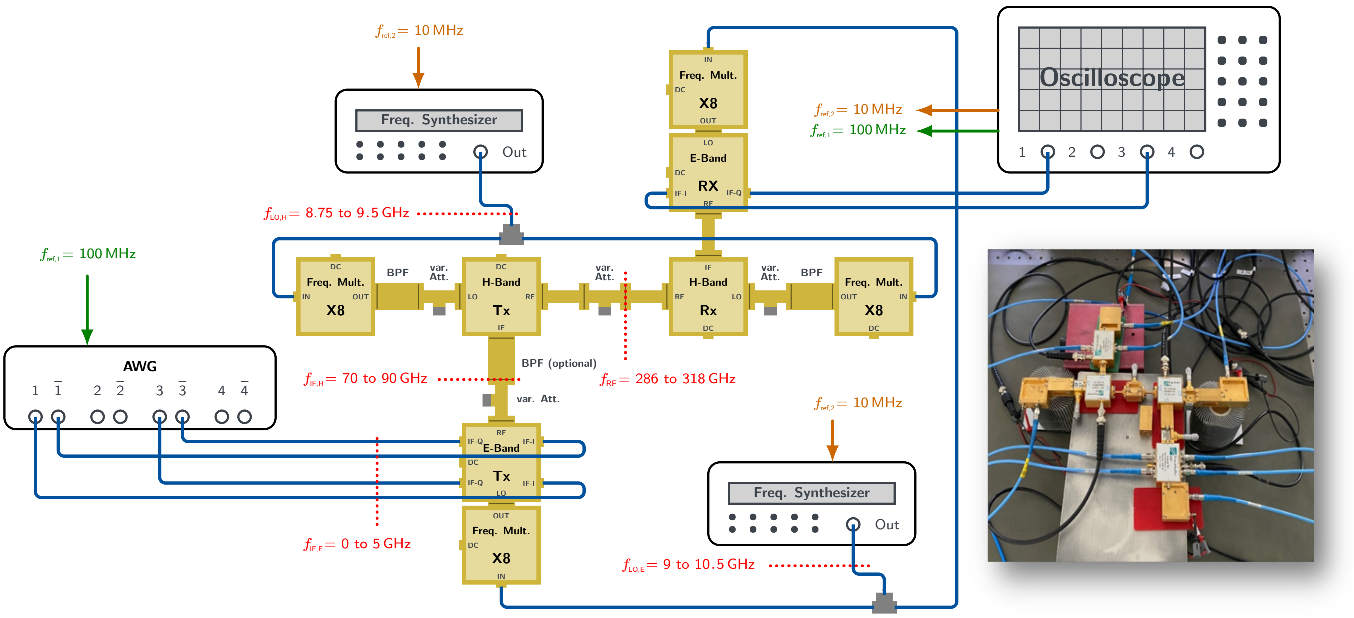

Fig. 6. Block diagram of the measurement setup used for transmission of complex modulated signals as well as photograph of the connected module chain.

and lower sideband contributions versus IF frequency of the E-band frequency extension at an exemplary LO frequency of 78.25 GHz and IF input power of –10 dBm. For the CW measurements only the differential in-phase (I) ports are fed with signals provided by an AWG. The differential quadrature (Q) ports are each terminated with coaxial 50 Ω loads.

B. Modulated Setup

In contrast to the CW measurement setup, a custom E-band frequency extensions is also used at the receiver side to down-convert broadband modulated signals from the H-band IF interface. The corresponding E-band Rx is realized by a highly linear resistive quadrature down-conversion mixer

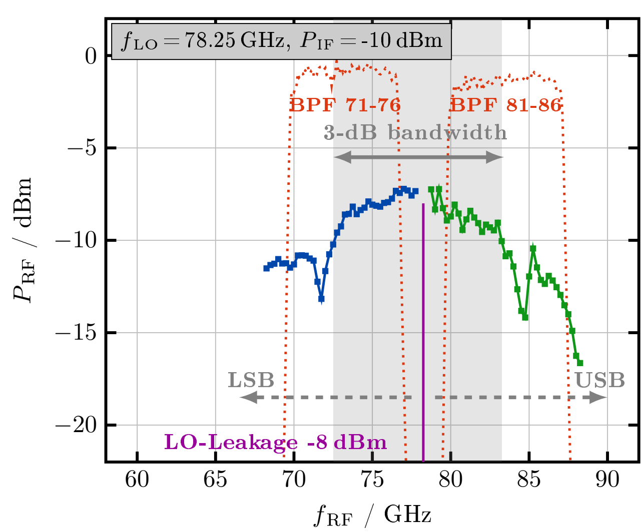

Fig. 7. RF output power of the E-band Tx at a f_{LO} of 78.25 GHz and P_{IF} of –10 dBm as a function of IF frequency as well as operating bands of the two available BPFs.

with a CG of –12 dB and an input-related 1dB compression point ICP_{1dB} beyond 0 dBm over the whole frequency range. With the expected input power from the H-band receiver not exceeding –15 dBm, linear operation with sufficient back-off from the ICP_{1dB} is ensured in all measurements. Again, the LO signals for the RF as well as the IF system are generated electronically using two frequency synthesizers, resulting in a coherent setup for each of the systems. As shown in Fig. 6 a real-time oscilloscope with 80 GSa/s and 20 GHz bandwidth is used to capture the I and Q baseband waveforms. To extract constellation diagrams, EVM and other metrics offline signal processing is performed using a vector signal analyzer software. The generation of the modulated waveforms is performed by an AWG with 64 GSa/s using pseudo-random bit sequences with a length of 2^{15} bits. Adjusting the dynamic range of the AWG to suit the input power range of the frequency extension, 5 dB fixed coaxial attenuators are used at the ports of the AWG. To compensate for cable loss and channel skew, an in-system calibration is performed from DC up to 10 GHz with the AWG and oscilloscope being directly connected. This way the residual EVM of the AWG signal is pushed below –40 dB for a 1 GBd QPSK reference signal.

IV. Measurement Results

Using the two setups explained in section III measurements are carried out to determine the optimum operating points and performance of the THz link.

A. Tx Linearity - CW

Based on the module characteristics presented in section II and therefore known CG at corresponding LO and IF frequency combinations measurements are carried out to determine the linearity of the transmitter using the CW measurement scenario. Therefore the IF signal power at the H-band Tx is swept from approximately –18 to –2 dBm as well

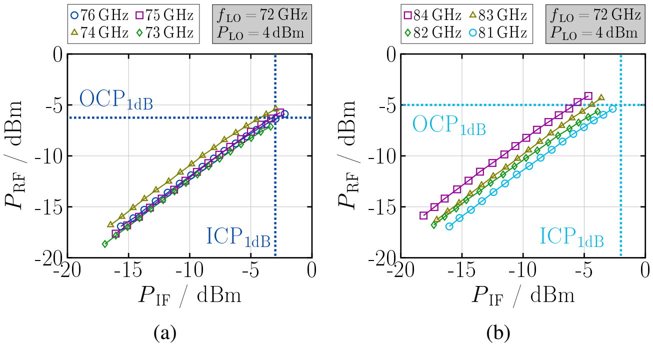

Fig. 8. Measured Tx output power as a function of the IF input power at $f_{LO} = 72$ GHz at several IF frequencies.

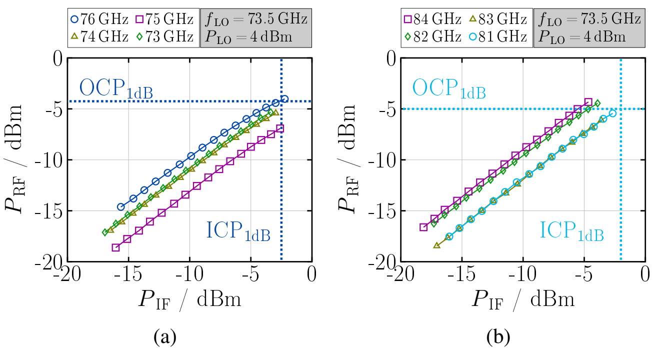

Fig. 9. Measured Tx output power as a function of the IF input power at $f_{LO} = 73.5$ GHz at several IF frequencies.

as the IF frequency using four different frequencies for each of the BPF passbands. The RF attenuation is set to a fixed level which ensures linear Rx operation. The corresponding curves are recorded for LO frequencies of 72 and 73.5 GHz as shown in Figs. 8 and 9. All four data sets show a strong linear behavior over all measured frequencies with the ICP_{1dB} lying in the range of –2 to –3 dBm for the marked IF frequencies of 76 and 81 GHz.

B. Rx Sensitivity - CW

By using fixed IF input power of –8 dBm to the H-band Tx, and therefore ensuring linear operation, the RF attenuation is varied manually via the tuneable WR-3.4 attenuator between approximately 30 and 10 dB. This way the sensitivity curves for the receiver, displayed in Figs. 10 and 11 are determined in analogy to the frequency sweeps performed for the Tx linearity characterization. Slight deviations in the obtained results between the characterization versus frequency and the linearity and sensitivity curves are related to tolerances of the manual adjustment of the variable attenuator. Within all four data sets the CG varies between 3 to 5 dB with the ICP_{1dB} varying between –18 and –24 dBm of RF input power for the marked IF frequencies of 76 and 81 GHz.

C. Modulated Waveforms

The measurements using modulated waveforms are evaluated using EVM as a performance metric. All presented

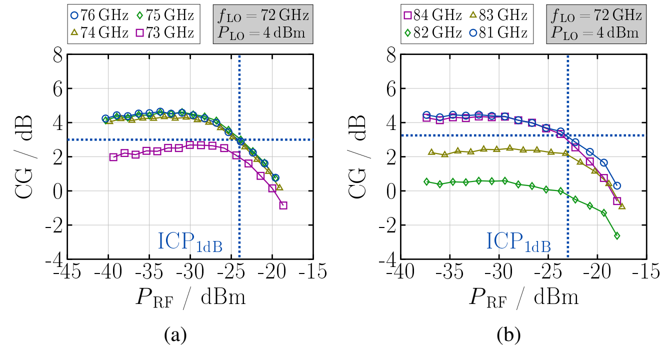

Fig. 10. Measured Rx CG as a function of RF input power at a f_{LO} of 72 GHz and different IF frequencies.

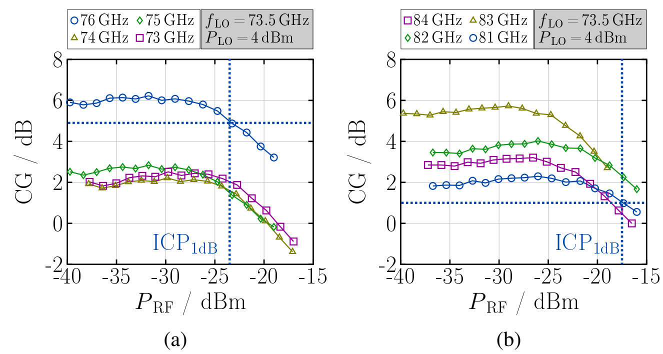

Fig. 11. Measured Rx CG as a function of RF input power at a f_{LO} of 73.5 GHz and different IF frequencies.

EVM values are normalized to the constellation's maximum amplitude and are received with frequency equalization being applied during post-processing.

Theoretical derivation of required back-off: To derive the optimum operating point of the Tx and Rx modules in order to achieve the best signal quality, at first a theoretical derivation of the required back-off from the ICP_{1dB} is conducted. This back-off is required due to the varying peak-to-average power ratios (PAPR) of the used quadrature modulation schemes. In case of phase-shift keying (PSK) modulations, such as QPSK and 8-PSK, the PAPR is 0 dB since there is only one amplitude level required. For even-order m-QAM modulations the

$$\mathrm{PAPR} = \frac{P_{\mathrm{peak}}}{P_{\mathrm{rms}}} = \frac{a_n^2}{\frac{1}{m}\sum_{i=1}^{n} a_i^2 \cdot n_i} \tag{1}$$

with respect to the total number of symbols in the constellation m, the used amplitude levels a_{i} weighted by the number of symbols n_{i} landing on the respective level. This calculation is valid under the assumption of equal probability of all symbols and therefore equal contribution of each symbol to the average signal power. With a normalized peak amplitude of 1 as indicated in Fig. 12 for 16-QAM modulation the corresponding PAPR is calculated to

$$\mathrm{PAPR}_{\text{16-QAM,dB}} = 10 \cdot \log\left(\frac{9}{5}\right) = 2.55\,\mathrm{dB} \tag{2}$$

indicating the minimum required back-off from the ICP_{1dB} compression point in order to not compress any symbol due to non-linear behavior of the device. Similarly the values for 64-QAM and 256-QAM are derived leading to 3.7 dB and 4.2 dB respectively.

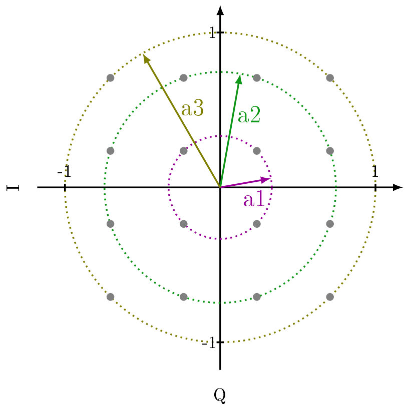

Fig. 12. Ideal 16-QAM constellation diagram as exemplary basis for the theoretical derivation of the PAPR of the signal.

D. Tx Linearity - Modulated

In order to determine the optimum operating point for future wireless transmission experiments, the transmitter performance is evaluated using complex modulated waveforms. First, the IF input power is swept in the range of –13 to –2 dBm applying QPSK, 8-PSK and 16-QAM signals with a baudrate of 1 GBd in order to determine the required back-off from the 1dB compression point to achieve minimum signal distortion. This is done for LO frequencies of 72 and 73.5 GHz as depicted in Fig. 13. To minimize the signal impairments arising from the frequency extension, such as LO leakage and spurious tones from the LO generation, a single-sideband (SSB) approach is chosen for those measurements. Therefore the IF signals are centered at 75.825 GHz and at 80.675 GHz when the 71 - 76 GHz and 81 - 86 GHz BPF is used respectively by applying a frequency offset in the signal generation. While for QPSK and 16-QAM the theoretically calculated required minimum back-off of 2.55 and 0 dB is verified, for 8-PSK modulation also a significant back-off of around 2.5 dB is indicated.

E. Rx Sensitivity - Modulated

Similarly to the characterization of the Tx the Rx module is evaluated by the transmission of 1 GBd signals using QPSK, 8-PSK and 16-QAM modulations. With a fixed Tx RF power of around –10 dBm, the RF attenuation is swept between approximately 30 and 10 dB. The resulting curves are shown in Fig. 14 with both indicating similar back-off requirements with respect to the applied modulation scheme. However, it has to be considered that the resolution and precision of the varied attenuation are subject to tolerances of 1 dB due to manual adjustment.

F. Maximum and IEEE802.15.3d Performance

In order to demonstrate the use of larger bandwidths, the baudrate is varied from 1 to 4 GBd using 16-QAM modulation. Considering a degradation of the SNR by ideally 3 dB per bandwidth doubling the minimum achievable EVM is increased. This behavior is observed in the measurement data as it is shown in Fig. 15 for LO frequencies of 72 and 73.5 GHz. The overall better signal quality is achieved with an LO frequency of 72 GHz compared to 73.5 GHz where the minimum EVM for a 4 GBd signal is 5 dB worse.

Table I additionally lists selected transmission results that have been achieved. The maximum data rate of 32 Gbit/s is achieved using 32-QAM modulation with a baudrate of 6.4 GBd while the maximum spectral efficiency is reached

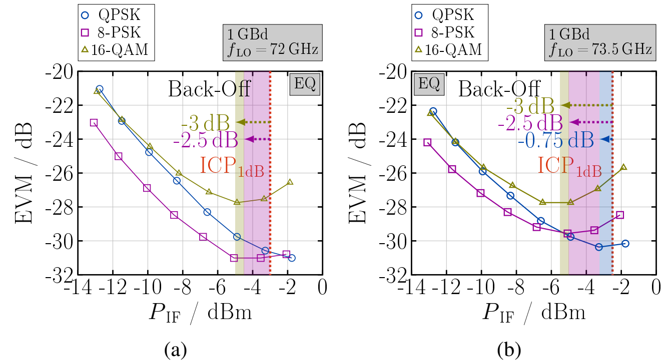

Fig. 13. Measured EVM of 1 GBd modulated signals centered at f_{IF} = 75.825 GHz as a function of IF input power at a) f_{LO} = 72 GHz and b) f_{LO} = 73.5 GHz.

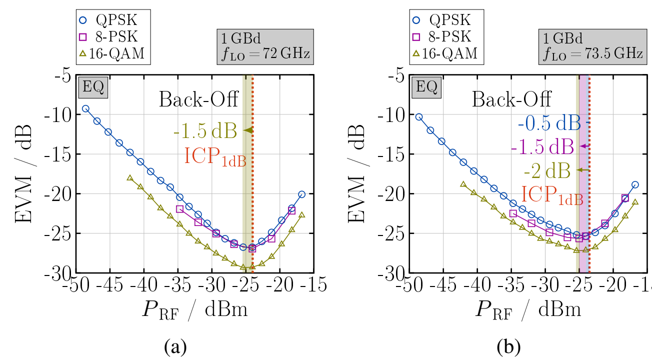

Fig. 14. Measured EVM of 1 GBd modulated signals centered at f_{IF} = 75.825 GHz as a function of the receiver RF input power at a) f_{LO} = 72 GHz and b) f_{LO} = 73.5 GHz.

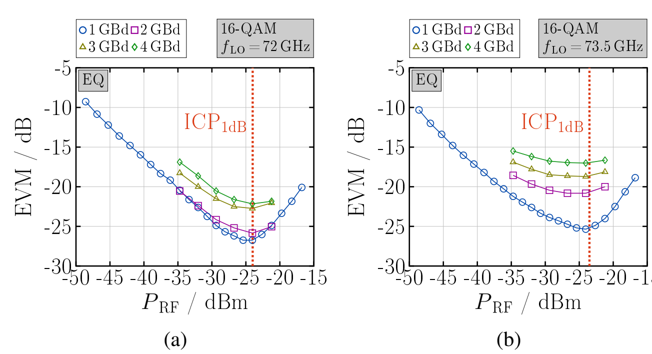

Fig. 15. Measured EVM 16-QAM signals as a function of the receiver RF input power and baudrate at a) f_{LO} = 72 GHz and b) f_{LO} = 73.5 GHz.

with 256-QAM modulation and a baudrate of 1 GBd resulting in data rate of 8 Gbit/s. Additionally, the link is evaluated for IEEE802.15.3d compliance by addressing several channels with bandwidths ranging from 2.16 GHz to 8.64 GHz with the latter one being limited by the bandwidth of the IF frequency extension. In channels 25 and 26 transmissions using 64-QAM and 128-QAM have been conducted which indicates the link's capability to also cope with typical E-band modems using channels with bandwidths up to 2 GHz and modulation schemes as high as 128-QAM. Furthermore, transmissions performed using channels 44 and 54 prove the compatibility with larger bandwidths using more robust modulation schemes like 8-PSK and 16-QAM. The link's operation in a simplex short-range wireless transmission scenario is successfully demonstrated in [17] where baseband modems are used in conjunctions with the same E-band frequency extensions to perform a real-time data transmission over a distance of 1.5 m. With respect to future IEEE802.15.3d applications, where multiple E-band modems will be used per link terminal, channel aggregation is of equal importance as the real-time capability of the RF hardware. The latter is successfully demonstrated in [18] where two pairs of the presented Tx and Rx modules are used to form a real-time full-duplex wireless link in conjunction with a set of commercial E-band modems, achieving a maximum throughput of 11.09 Gbit/s using 64-QAM modulation. To demonstrate channel aggregation capability, 16-QAM modulation is applied simultaneously in channels 24, 25, 26 and 27 with center frequencies of 303.48, 305.64, 307.8 and 309.96 GHz a combined data rate of 25.6 Gbit/s is achieved as displayed in Fig. 16. The decreasing signal power in channel 27 is mainly related to the IF frequency extension reaching its bandwidth limit where a significantly reduced conversion gain is observed. However, all four channels are recovered with an SNR between 14.4 and 17.5 dB as well as EVM values between –17 and –20.1 dB. Comparable bandwidth limitations by the IF frequency extension are observed in [12] and [13], where X-band mixers are used together with H-band Tx and Rx modules to implement a superheterodyne link architecture. This way a maximum data rate of 24 Gbit/s was achieved using 16-QAM modulation, which is slightly lower than the 25.6 Gbit/s shown in this scenario. Higher data rates up to 60 Gbit/s are achieved in [12] and [13] by generating and modulating the IF signals onto a 10 GHz carrier by the AWG internally. This is not an option for IF signals at E-band frequencies used in this work as this would require ultra-fast digital-to-analog converters. With the actual IF bandwidth of the H-band Tx and Rx extending over the entire E-band, the link is in principle capable of sustaining a higher number of aggregated IF channels and, thus, higher aggregate data rates. Besides the integration of already existing links, operating based on E-band frequency standards, this is why moving to higher intermediate frequencies for superheterodyne THz links is advantageous. The aggregation of multiple E-band modems per link terminal will be the focus of our future work.

V. Discussion

With the gained measurement results the link's capabilities in a wireless transmission scenario can be estimated in terms of maximum transmission distance at optimum signal quality. Taking into account, on one hand, the IF input and corresponding RF output power levels of the transmitter and, on the other hand, the maximum RF input power levels at the receiver where the EVM is minimized, the targeted loss between Tx and Rx aiming for optimum signal quality is estimated. With the optimum Tx RF output power and the Rx RF input power lying in the range of –8 dBm and –24 dBm respectively, with slight dependency on the used modulation scheme, the loss target is calculated to 16 dB. Thus for a short-range wireless transmission scenario using commercial WR-3.4 horn antennas with an antenna gain of 25 dBi, the corresponding tolerable free-space path loss (FSPL) is 66 dB. With that the optimum transmission distance

$$20 \cdot \log(d) = \mathrm{FSPL} - 20 \cdot \log(f_c) - 20 \cdot \log\left(\frac{4\pi}{c}\right) + G_{\mathrm{Tx+Rx}} \quad (3)$$

is derived to be 0.16 m for a center frequency of 300 GHz, neglecting additional impairments like feeder loss. In order to increase this distance additional amplifiers like [4] will be used at the transmitter which enlarges the loss margin potentially by about 6 to 10 dB, depending on the required back-off from the $\mathrm{ICP}_{1\mathrm{dB}}$ of the amplifier, resulting in at least a doubling of the distance. However to match the high amplifier gain with the optimum output power of the Tx, an additional attenuator is required in between both modules. By additionally enlarging the antenna gain to 55 dBi per terminal using Cassegrain antennas as reported in [19], an optimum operation distance in the range of 150 m is predicted, already subtracting a 6 dB margin which accounts for feeder loss as well as pointing loss due to the high directivity of the system.

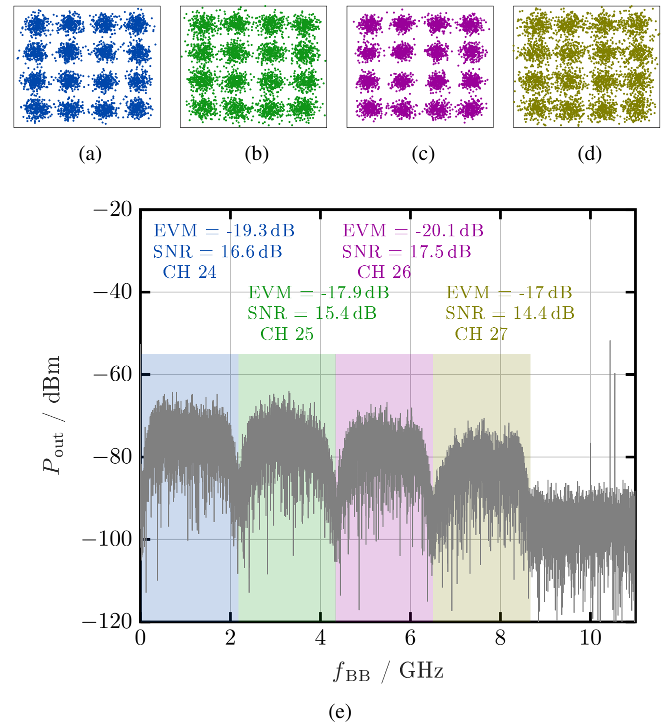

Fig. 16. Measured received spectrum e) and Constellations a) - d) of four aggregated 1.6 GBd 16-QAM signals using channels 24, 25, 26 and 27 in the RF domain.

TABLE I
SELECTED RESULTS OF MAXIMUM PERFORMANCE AND IEEE802.15.3D COMPLIANCE ACHIEVED IN THE PRESENTED SETUP.

	Maximum performance		**IEEE802.15.3d**			
Channel ID	-	-	44	54	25	26
$f_{\mathrm{IF,center}}$ **/ GHz**	79.1	79.25	85.7	79.1	84.6	84.6
$f_{\mathrm{RF,center}}$ **/ GHz**	301.2	304.25	302.4	300.2	305.6	307.8
Bandwidth / GHz	8.64	1.35	4.32	8.64	2.16	2.16
Data Rate / Gbit/s	32	8	9.6	25.6	9.6	11.2
Modulation Scheme	32-QAM	256-QAM	8-PSK	16-QAM	64-QAM	128-QAM
Constellation	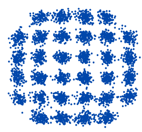	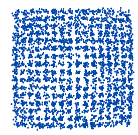	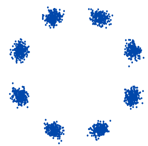	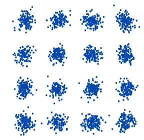	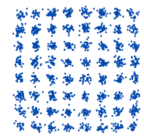	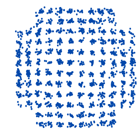
EVM / dB	–23.6	–30.8	–20.9	–21.4	–27.1	–30.5
SNR / dB	19.6	26.3	20.6	19	23.5	25.6

VI. STATE OF THE ART

Table II lists state-of-the-art transmission experiments using electronic THz transceivers for wireless communication with RF operating frequencies around 300 GHz and suitable for IEEE802.15.3d applications. While only [20] uses a direct-conversion architecture, more often a heterodyne or super-heterodyne link topology is implemented. This work is the one demonstrating the highest IF frequency range, spanning over the whole E-band from 60 to 90 GHz, offering the direct embedding of already existing links operating in the 71 - 76 or 81 - 86 GHz frequency bands into a THz front- or backhaul scenario. The link in [20] uses the same 35 nm InGaAs mHEMT technology as this work and reports on the largest experimentally verified transmission distance of 500 m and 1 km, achieving data rates of 22 and 2 GBd respectively using 16-QAM modulation. Using lesser order schemes like 4-QAM data rates of 42 and 28 GBd over the respective distances. However, it has to be noted that additional DSP measures like a linear pre-distortion are applied in order to improve the link's performance. As reported in [21] and [22] transceivers using CMOS technologies achieve data rates of 80 and 34 Gbit/s respectively. The first uses a quadrature mixer with an LO of 133 GHz followed by a frequency doubler to translate baseband signals to the RF domain and achieves its maximum data rate using 16-QAM. The latter also uses a superheterodyne architecture with IF frequencies between 50 and 70 GHz. Achieving a comparable maximum data rate of 34 Gbit/s but using 17 GBd QPSK, it has to be noted that the corresponding spectral efficiency is significantly lower compared to this work's 32 Gbit/s using 6.4 GBd 32-QAM. Due to comparably small transmit power levels the corresponding achievable transmission distances are significantly shorter compared to links based on III-V semiconductor technologies. The overall highest reported data rate of 120 Gbit/s is reported in [7] using 16-QAM.

VII. CONCLUSION

In this paper, we successfully demonstrated the operation of a superheterodyne THz link targeting IEEE802.15.3d applications. First, the CW characterization of the Tx and Rx modules has been performed to extract the respective $\mathrm{ICP}_{1\mathrm{dB}}$ as a performance metric to determine the optimum operating point for transmission experiments using modulated signals. Second, experiments with signals using various complex modulation schemes are carried out using EVM as a performance metric. The obtained results for a minimum EVM are in good accordance with a theoretical derivation of the required back-off depending on the employed modulation scheme. It has been shown that the link offers sufficient linearity and dynamic range to transmit signals with spectral efficiency of up to 8 bits/Hz using 256-QAM modulation. Applying 32-QAM modulation the highest demonstrated data rate was 32 Gbit/s which however was mainly limited by the available IF frequency extension used for the characterization. Additionally, the compliance with the IEEE802.15.3d standard is tested over several single channels as well as with the aggregation of four channels with 2.16 GHz of individual bandwidth. This promises the successful future operation of the Tx and Rx modules embedded in a real-time wireless backhaul scenario. To the best of the author's knowledge this is the first demonstration of a superheterodyne THz link operating around 300 GHz with IF frequency capabilities extending over the whole E-band from 60 to 90 GHz which offers the embedding of already existing links operating in the 71 - 76 or 81 - 86 GHz frequency bands.

ACKNOWLEDGMENT

The authors would like to thank their colleagues at Fraunhofer IAF for excellent wafer growth, processing, characterization and packaging.

REFERENCES

[1] A.-A. A. Boulogeorgos, A. Alexiou, T. Merkle, C. Schubert, R. Elschner, A. Katsiotis, P. Stavrianos, D. Kritharidis, P.-K. Chartsias, J. Kokkoniemi, M. Juntti, J. Lehtomaki, A. Teixeira, and F. Rodrigues, "Terahertz Technologies to Deliver Optical Network Quality of Experience in Wireless Systems Beyond 5G," *IEEE Communications Magazine*, vol. 56, no. 6, pp. 144–151, 2018.
[2] *World Radiocommunication Conference 2019 - Final Acts*, 2019.

TABLE II
COMPARISON OF STATE-OF-THE-ART ELECTRONIC THZ TRANSCEIVERS OPERATING AT A CENTER FREQUENCY AROUND 300 GHZ.

	RF Freq. / GHz	Technology	Data Rate / Gbit/s	Modulation	Transm. Distance / m	Architecture	IF Freq. / GHz
This Work	285 - 312	35 nm InGaAs	32	32-QAM	back-to-back / 150*	superheterodyne	60 - 90
[20]	272 - 322	35 nm InGaAs	96 / 8	16-QAM	500 / 1000	direct-conversion	0 - 25
[21]	255 - 275	40 nm CMOS	80	16-QAM	0.03	heterodyne	0 - 20**
[22]	278 - 304	65 nm CMOS	34	QPSK	0.01	superheterodyne	50 - 70
[7]	275 - 302	80 nm InP	120	16-QAM	9.8	heterodyne	0 - 20

*calculated **simulated

[3] *IEEE Standard for High Data Rate Wireless Multi-Media Networks–Amendment 2: 100 Gb/s Wireless Switched Point-to-Point Physical Layer*, Std.

[4] L. John, A. Tessmann, A. Leuther, P. Neininger, T. Merkle, and T. Zwick, "Broadband 300-GHz Power Amplifier MMICs in InGaAs mHEMT Technology," *IEEE Transactions on Terahertz Science and Technology*, vol. 10, no. 3, pp. 309–320, 2020.

[5] A. Tessmann, A. Leuther, S. Wagner, H. Massler, M. Kuri, H.-P. Stulz, M. Zink, M. Riessle, and T. Merkle, "A 300 GHz Low-Noise Amplifier S-MMIC for Use in Next-Generation Imaging and Communication Applications," in *2017 IEEE MTT-S International Microwave Symposium (IMS)*, 2017, pp. 760–763.

[6] P. Rodríguez-Vázquez, J. Grzyb, B. Heinemann, and U. R. Pfeiffer, "Performance Evaluation of a 32-QAM 1-Meter Wireless Link Operating at 220–260 GHz with a Data-Rate of 90 Gbps," in *2018 Asia-Pacific Microwave Conference (APMC)*, 2018, pp. 723–725.

[7] H. Hamada, T. Tsutsumi, H. Matsuzaki, T. Fujimura, I. Abdo, A. Shirane, K. Okada, G. Itami, H.-J. Song, H. Sugiyama, and H. Nosaka, "300-GHz-Band 120-Gb/s Wireless Front-End Based on InP-HEMT PAs and Mixers," *IEEE Journal of Solid-State Circuits*, vol. 55, no. 9, pp. 2316–2335, 2020.

[8] A. Leuther, A. Tessmann, M. Dammann, H. Massler, M. Schlechtweg, and O. Ambacher, "35 nm mhemt technology for thz and ultra low noise applications," in *2013 International Conference on Indium Phosphide and Related Materials (IPRM)*, 2013, pp. 1–2.

[9] ITU-R, "Radio-frequency channel and block arrangements for fixed wireless systems operating in the 71-76 and 81-86 ghz bands," Recommendation, Mar. 2012.

[10] ETSI, "Fixed Radio Systems; Characteristics and requirements for point-to-point equipment and antennas; Part 2: Digital systems operating in frequency bands from 1 GHz to 86 GHz; Harmonised Standard for access to radio spectrum," Standard, Jun. 2021.

[11] "MaxLinear 20 Gbps Millimeter MXL85110 MODEM Enables Backhaul Connectivity for Siklu EtherHaul™ Product Family," Press Release, Apr. 2020. [Online]. Available: https://www.siklu.com/press-release/maxlinear-modem-enables-backhaul-connectivity-for-siklu-etherhaul-product-family/

[12] I. Dan, G. Ducournau, S. Hisatake, P. Szriftgiser, R.-P. Braun, and I. Kallfass, "A Superheterodyne 300 GHz Wireless Link for Ultra-Fast Terahertz Communication Systems," *International Journal of Microwave and Wireless Technologies*, vol. 12, no. 7, p. 578–587, 2020.

[13] ——, "A Terahertz Wireless Communication Link Using a Superheterodyne Approach," *IEEE Transactions on Terahertz Science and Technology*, vol. 10, no. 1, pp. 32–43, 2020.

[14] B. Schoch, A. Tessmann, A. Leuther, S. Wagner, and I. Kallfass, "300 GHz broadband power amplifier with 508 ghz gain-bandwidth product and 8 dbm output power," in *2019 IEEE MTT-S International Microwave Symposium (IMS)*, 2019, pp. 1249–1252.

[15] I. Dan, C. Grötsch, L. John, S. Wagner, A. Tessmann, and I. Kallfass, "A Superheterodyne 300 GHz Transmit Receive Chipset for Beyond 5G Network Integration," in *2021 European Microwave Week (EuMW)*, 2022.

[16] P. Harati, B. Schoch, A. Tessmann, D. Schwantuschke, R. Henneberger, H. Czekala, T. Zwick, and I. Kallfass, "Is E-Band Satellite Communication Viable?: Advances in Modern Solid-State Technology Open Up the Next Frequency Band for SatCom," *IEEE Microwave Magazine*, vol. 18, no. 7, pp. 64–76, 2017.

[17] D. Wrana, L. John, B. Schoch, S. Wagner, and I. Kallfass, "Short Range Wireless Transmission Using a 295–315 GHz Superheterodyne Link Targeting IEEE802.15.3d Applications," in *2021 European Microwave Week (EuMW)*, 2022.

[18] D. Wrana, Y. Leiba, L. John, B. Schoch, A. Tessmann, and I. Kallfass, "Short-Range Full-Duplex Real-Time Wireless Terahertz Link for IEEE802.15.3d Applications," in *2022 IEEE Radio and Wireless Symposium (RWS)*, 2022, pp. 94–97.

[19] J. Antes, F. Boes, T. Messinger, U. J. Lewark, T. Mahler, A. Tessmann, R. Henneberger, T. Zwick, and I. Kallfass, "Multi-Gigabit Millimeter-Wave Wireless Communication in Realistic Transmission Environments," *IEEE Transactions on Terahertz Science and Technology*, vol. 5, no. 6, pp. 1078–1087, 2015.

[20] C. Castro, R. Elschner, T. Merkle, C. Schubert, and R. Freund, "Long-range High-Speed THz-Wireless Transmission in the 300 GHz Band," in *2020 Third International Workshop on Mobile Terahertz Systems (IWMTS)*, 2020, pp. 1–4.

[21] S. Lee, R. Dong, T. Yoshida, S. Amakawa, S. Hara, A. Kasamatsu, J. Sato, and M. Fujishima, "9.5 An 80Gb/s 300GHz-Band Single-Chip CMOS Transceiver," in *2019 IEEE International Solid- State Circuits Conference - (ISSCC)*, 2019, pp. 170–172.

[22] I. Abdo, T. Fujimura, T. Miura, K. K. Tokgoz, H. Hamada, H. Nosaka, A. Shirane, and K. Okada, "A 300GHz Wireless Transceiver in 65nm CMOS for IEEE802.15.3d Using Push-Push Subharmonic Mixer," in *2020 IEEE/MTT-S International Microwave Symposium (IMS)*, 2020, pp. 623–626.

Dominik Wrana received the Master of Science degree in Electrical Engineering from Reutlingen University, Germany in 2019. Since 2019, he has been with the Institute of Robust Power Semiconductor Systems (ILH), University of Stuttgart, Germany as a research and teaching assistant. His current research focuses on the system- to circuit-level engineering for ultra-broadband wireless communications systems operating at millimeter and sub-millimeter wave frequencies. He is involved in the design and characterization of monolithic integrated circuits as well as system-level performance analysis and optimization.

Laurenz John Laurenz John received the Master of Science (M.Sc.) and Ph.D. (Dr.-Ing) degrees in Electrical Engineering and Information Technologies from the Karlsruhe Institute of Technology (KIT), Karlsruhe, Germany, in 2016 and 2021, respectively. He is currently an RF design engineer and project leader with Fraunhofer IAF, Freiburg, Germany. Since 2016, he has been involved in the design and characterization of InGaAs-channel HEMT devices and integrated circuits on GaAs and Si substrates for wireless applications up to 800 GHz. His current research interests include IC and package design for radar, communication and quantum computing applications at mm-wave and THz frequencies. .

Benjamin Schoch received his M.Sc. degree in power and microelectronics from Reutlingen University, Germany in 2016 in the frame of the Robert Bosch Center for Power Electronics (rbz). Since 2016 he has been a research and teaching assistant at the Institute of Robust Power Semiconductor Systems, University of Stuttgart, Germany in the area of millimeter and sub-millimeterwave monolithic integrated circuits for broadband communication and radar imaging with a main research focus on power amplifier.

Sandrine Wagner received a Bachelor of Science in Electronics and Informatics from the University of Mulhouse, France in 1989. She joined Micronas GmbH in Freiburg, Germany in 1989 where she was responsible for layout and physical verification of large scale integrated semi-conductor devices. In 2010 she joined the Fraunhofer Institute for Applied Solid State Physics (IAF), Freiburg, Germany. Her main interest is the measurement of high frequency non-linear circuits.

Ingmar Kallfass received the Dipl.-Ing. degree in Electrical Engineering from University of Stuttgart in 2000, and the Dr.-Ing. degree from University of Ulm in 2005. In 2001, he worked as a visiting researcher at the National University of Ireland, Dublin. In 2002, he joined the department of Electron Devices and Circuits of University of Ulm as a teaching and research assistant. In 2005, he joined the Fraunhofer Institute for Applied Solid-State Physics. From 2009 to 2012, he was a professor at the Karlsruhe Institute of Technology. Since 2013, he holds the chair for Robust Power Semiconductor Systems at the University of Stuttgart, where his major fields of research are compound semiconductor-based circuits and systems for power and microwave electronics.